coatings

Article

Experimental Analysis of Bearing Capacity of Basalt Fiber Reinforced Concrete Short Columns under Axial Compression

Xinzhong Wang [1,2], Yiming Yang [1,*], Rihua Yang [1] and Peng Liu [3,*]

[1] School of Civil Engineering, Hunan City University, Yiyang 413000, China; zhong811@126.com (X.W.); yrhzjh@163.com (R.Y.)
[2] Hunan Engineering Research Center of Structural Safety and Disaster Prevention for Urban Underground Infrastructure, Hunan City University, Yiyang 413000, China
[3] School of Civil Engineering, Central South University, Changsha 410013, China
* Correspondence: yangyiming@hncu.edu.cn (Y.Y.); 2015038@csu.edu.cn (P.L.); Tel.: +86-18173116706 (Y.Y.); +86-15116277646 (P.L.)

Abstract: Adding basalt fiber to concrete can improve the mechanical properties of concrete, and it is also one of the best ways to enhance the ultimate bearing capacity of concrete structure. In this paper, the construction performance and the compressive strength of basalt-fiber-reinforced concrete (BFRC) with five kinds of fiber lengths and eight kinds of fiber volume content subjected to an axial load are systematically investigated. The optimum fiber length and fiber volume content are obtained by comprehensively considering the construction performance and compressive strength. Moreover, the prediction model and finite element analysis method of the ultimate bearing capacity of basalt-fiber-reinforced concrete are developed. The results show that the optimum fiber length is about 12–24 mm and the fiber volume content is 0.15%. Adding an appropriate amount of basalt fiber can effectively improve the ultimate bearing capacity of concrete short columns, with maximum and average increases of 28% and 24%, respectively. In addition, the comparison with the experimental results shows that both the proposed prediction method and the finite element modeling method have good applicability, and they can be used to predict the ultimate bearing capacity of the BRFC short columns in practical engineering.

Keywords: basalt-fiber-reinforced concrete; concrete compressive strength; construction performance; ultimate bearing capacity; finite element analysis

check for updates

Citation: Wang, X.; Yang, Y.; Yang, R.; Liu, P. Experimental Analysis of Bearing Capacity of Basalt Fiber Reinforced Concrete Short Columns under Axial Compression. *Coatings* **2022**, *12*, 654. https://doi.org/10.3390/coatings12050654

Academic Editor: Paolo Castaldo

Received: 15 April 2022
Accepted: 9 May 2022
Published: 11 May 2022

1. Introduction

Reinforced concrete (RC) short columns are some of the most basic components in structural engineering and are widely used in bridge piers, building frames, workshop columns, and other concrete structures. Their bearing capacity and durability are crucial to the safety, applicability, and economy of the entire structure. At present, they are effective at improving the mechanical properties of concrete by adding chopped fibers, such as steel fibers [1], glass fibers [2], synthetic fibers [3,4], basalt fibers [5], carbon fibers [6,7], etc. This is mainly because the appropriate fiber length and fiber volume contents can effectively combine with the weak matrix in concrete, so as to better control the development of internal cracks in concrete and finally improve the mechanical properties of concrete [8]. However, different types of fiber-reinforced concrete have different mechanical properties or application characteristics. For example, adding steel fiber to concrete can improve the toughness and tensile strength of concrete, but the processability and corrosion resistance of steel fiber are not good. Adding glass fiber into concrete can enhance the toughness of concrete, but its long-term strength will be reduced. Although carbon fiber has the characteristics of hardness and high strength, its use cost is high [9]. In view of the above problems, basalt fiber, which has the advantages of high tensile strength, high elastic modulus, corrosion resistance, good chemical stability, environmental protection, no pollution, and low cost, is gradually being studied [10–13]. Therefore, it is urgent to study the mechanical properties of the basalt-fiber-reinforced concret (BRFC) and its corresponding concrete members.

To date, researchers have mainly studied the reinforcement effect of basalt fiber and the mechanical properties of corresponding concrete. For example, both Ayub et al. [14] and Wang et al. [15] found that adding basalt fiber to concrete can improve its strength, and the maximum increase in compressive strength of basalt fiber concrete is 47.5%. According to previous research by Monaldo et al. [16], the tensile strength of concrete can be increased by 22.9% after 28 d by using 0.6% basalt fiber. A few scholars have determined the optimum content of basalt fiber based on the mechanical properties of concrete after adding basalt fiber. Based on the strength test of concrete with two kinds of fiber lengths and five kinds of fiber volume contents, Sun et al. [17] found that BFRC with 2% fiber volume content and 6 mm fiber length achieve the maximum strength. Tumadhir [18] believed that the optimum fiber volume content is about 0.3%, from the perspective of obtaining maximum compressive strength. However, most of the above studies obtain the optimal fiber length or fiber volume content based on the mechanical properties of specimens corresponding to a few fiber lengths and do not consider the construction performance of concrete. Therefore, it is urgent to carry out the mechanical property test of concrete under various fiber lengths and fiber volume contents and comprehensively determine the reasonable fiber parameters in combination with the construction performance.

Other than BFRC specimens, some scholars have studied the mechanical properties of basalt fiber concrete members, but most of them have focused on basalt fiber concrete beams. Based on the experimental research on BFRC beams, both Zhang [19] and Wang et al. [20] found the addition of basalt fiber can effectively prevent the development of cracks in reinforced concrete flexural members. Alnahhal and Aljidda [21] studied the flexural behavior and ultimate capacity of the BFRC beams experimentally and analytically based on the test results of 16 BFRC beams. At present, although a few scholars have conducted preliminary research on the performance of the BRFC short columns, such as Zhu [22], the research results on the ultimate bearing capacity of the BRFC short columns are highly deficient, and the relevant bearing capacity prediction methods have not been proposed. Therefore, it is necessary to further study the variation law of the bearing capacity of the BRFC short columns and propose corresponding prediction methods.

The objective of this study is to analyze the bearing capacity of the BRFC short columns under axial compression. First, the optimum fiber length and fiber volume content are obtained based on the construction performance and the concrete compressive strength. Then, the results of the axial compression test of the BRFC short columns are analyzed in depth. Finally, the theoretical and finite element calculation method of the ultimate bearing capacity of the BFRC short column are proposed, and their effectiveness is verified based on the test results. Among them, determining the optimum characteristic parameters of basalt fiber by comprehensively considering the construction and mechanical properties of concrete and proposing the assessment method of the ultimate bearing capacity of the BRFC short columns are the novelties of this paper.

2. Materials

The ordinary portland cement with the type of P.O 42.5 was selected. The crushed stone adopted two kinds of crushed stone of 5–10 mm and 10–25 mm, at a ratio of 2:3, to form a continuous secondary distribution. The corresponding crush value was 10.5, the sand fineness modulus was 2.85, and tap water was used. No water reducer was used during construction. The mix proportion data are shown in Table 1. The short cut basalt fiber produced by Zhejiang Hengdian Shijin Basalt Fiber Co., Ltd. Jinhua, China is adopted. Five lengths of basalt fibers are shown in Figure 1. The physical and mechanical properties of basalt fiber include the fiber diameter of 17 μm; the fiber density of 2650 kg/m^3; the tensile strength of 3000 MPa; the elastic modulus of 90 GPa; and fiber lengths of 12 mm, 18 mm, 24 mm, 30 mm, and 36 mm, respectively, as shown in Table 2.

Table 1. The mixed proportion of the concrete.

Target Intensity	Water Cement Ratio	Sand Ratio/%	Cement (kg/m^3)	Water (kg/m^3)	Sand (kg/m^3)	Crushed Stone (kg/m^3)
C30	0.55	34	355	195	703	1147

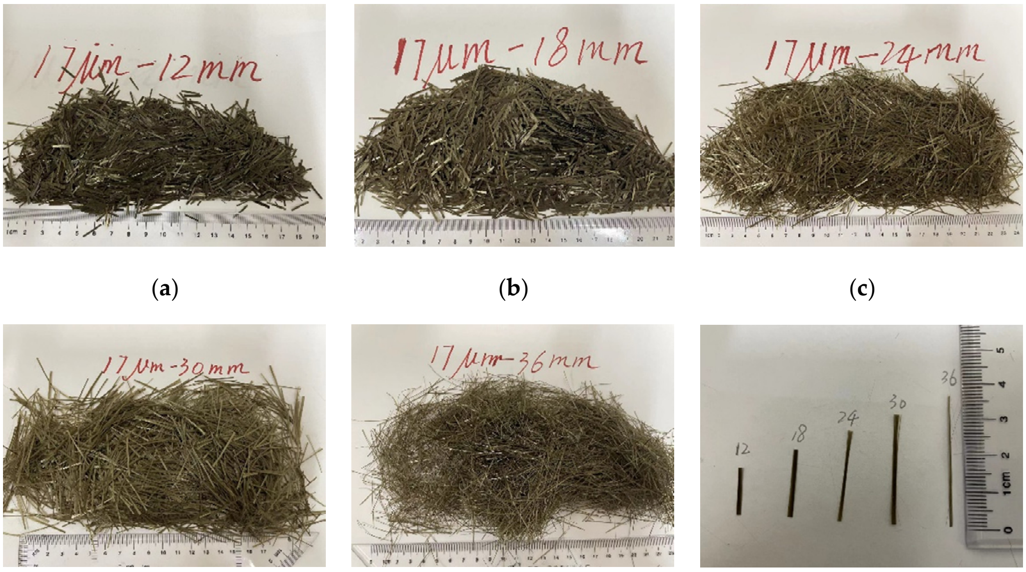

(**a**) (**b**) (**c**)

(**d**) (**e**) (**f**)

Figure 1. The five lengths of basalt fiber: (**a**) L = 12 mm; (**b**) L = 18 mm; (**c**) L = 24 mm; (**d**) L = 30 mm; and (**e**) L = 36 mm; and (**f**) a schematic diagram of the different fiber lengths.

Table 2. The physical and mechanical properties of the basalt fiber.

Index	Diameter (μm)	Length (mm)	Density (kg/m^3)	Tensile Strength (MPa)	Modulus of Elasticity (GPa)
Parameter	0.55	12/18/24/30/36	2650	3000	703

3. Construction Performance and Optimal Parameters of the BRFC

3.1. Construction Performance Test of the BRFC

The slump and expansion are selected here to analyze the construction performance of the BRFC, and the detailed test methods and procedures can be found in the Chinese specification of GB/T 50080-2016 [23]. A total of 13 groups of cube concrete specimens numbered ST1–ST13 are designed, and each group contains three parallel specimens. The STI, without adding fiber, is used as the reference specimen. Specimens ST2–ST6 are constructed using five kinds of basalt fibers with a fiber volume content of 0.15% and fiber lengths of 12 mm, 18 mm, 24 mm, 30 mm, and 36 mm. Five groups of the BRFC specimens with different fiber lengths are obtained to test the slump and expansion, and the average test results of each group of specimens are shown in Table 3. Specimens ST7–ST13 are constructed using seven kinds of basalt fibers with a fiber length of 12 mm and fiber volume contents of 0.075%, 0.10%, 0.15%, 0.20%, 0.25%, 0.30%, and 0.40%. The average test results of slump and expansion of ST7–ST13 are shown in Table 4. In order to better compare the difference between the slump and expansion of the BRFC and the ordinary concrete, the relative values of slump and relative expansion are calculated.

Table 3. The slump test results of the BRFC with different fiber lengths.

Group of Specimen	Fiber Length (mm)	Slump (mm)	Expansion (mm)	Relative Value of Slump (%)	Relative Value of Expansion (%)
ST1	0	30.4	61.5	100.0	100.0
ST2	12	27.8	53.4	91.4	86.8
ST3	18	25.7	48.6	84.5	79.0
ST4	24	23.2	43.2	76.3	70.2
ST5	30	24.7	47.1	81.2	76.6
ST6	36	26.8	49.4	85.1	80.3

Note: the relative value is the ratio of the measured value of the BRFC to that of the ordinary concrete.

Table 4. The slump test results of the BRFC with different fiber volume contents.

Group of Specimen	Fiber Volume Content (%)	Slump (mm)	Expansion (mm)	Relative Value of Slump (%)	Relative Value of Expansion (%)
ST1	0	30.4	61.5	100.0	100.0
ST7	0.075	28.2	56.3	92.8	91.5
ST8	0.10	27.8	54.2	91.4	88.1
ST9	0.15	25.4	52.1	83.6	84.7
ST10	0.20	23.1	43.4	76.0	70.6
ST11	0.25	20.2	38.3	66.4	62.3
ST12	0.30	18.3	32.4	60.2	52.7
ST13	0.40	15.8	30.1	52.0	48.9

As shown in Tables 3 and 4, the slump of the BRFC is lower than that of ordinary concrete. As the length of the added basalt fiber increases, the slump and expansion of the concrete first decreases and then increases. The slump and expansion of the BRFC is inversely correlated with the volume content of basalt fiber. This is due to the chaotic effect of basalt fibers, where a greater confinement effect on the concrete occurs with longer fiber and larger dosage and thus reduces the flow performance of the concrete. When the dosage is constant, the longer the fiber, the fewer the number of fibers, and thus the less restrictive the effect on the concrete.

3.2. Optimal Fiber Length and Fiber Volume Content

To further study the effect of fiber volume content on concrete compressive strength under different fiber lengths, we added BFRC specimens with a fiber length of 24 and fiber volume contents of 0, 0.075%, 0.10%, 0.15%, 0.20%, 0.25%, 0.30%, and 0.40% on the basis of ST1–ST13. Each case also contains three specimens. Then, based on the standard for the test methods of the mechanical properties of ordinary concrete (GB/T 50081-2002) [24], the 28 d compressive strength test is carried out on the cube concrete specimens with different fiber lengths and fiber volume contents, respectively. From the compressive failure modes of all specimens, the concrete specimens made an obvious cracking sound when they were damaged. The integrity of the BRFC specimen shows good resistance to damage regarding the rare cracking phenomenon. For the BFRC specimen that fails, the failure mode is brittle failure, although the characteristics of ductility are seen. The failure morphology of the BFRC specimens does not vary significantly with different fiber volume contents.

The compressive strength test results are presented in Figures 2 and 3. As indicated, with the increase of fiber length and fiber volume content, the concrete compressive strength basically conforms to the law of first increasing and then decreasing. This is mainly because under the action of short fiber length and small fiber volume content, the fiber distribution is more uniform, which can effectively prevent the generation of micro cracks in concrete, so as to improve the concrete compressive strength. For longer fiber length and larger fiber volume content, when they exceed a certain value, the fiber is easy to wind or agglomerate, which leads to the weakening of the connection effect between the fiber and the concrete matrix, thus leading to a failure to exert its reinforcing effect. It is worth noting that the average test strength of this group of concrete specimens with a fiber length of 36 mm does not comply with the above law, which may be caused by the good dispersion of fibers in the concrete. In addition, it can also be seen from Figures 2 and 3 that the concrete compressive strength is relatively high when the fiber length is about 12–24 mm and the fiber volume content is 0.15%. It is worth noting that although the construction performance cannot reach the optimal state under the effect of the above fiber length and content, it is sufficient to meet the normal construction needs. Thus, this paper focuses on the performance index of concrete compressive strength, and then obtains the optimal fiber length and fiber volume based on the analysis results.

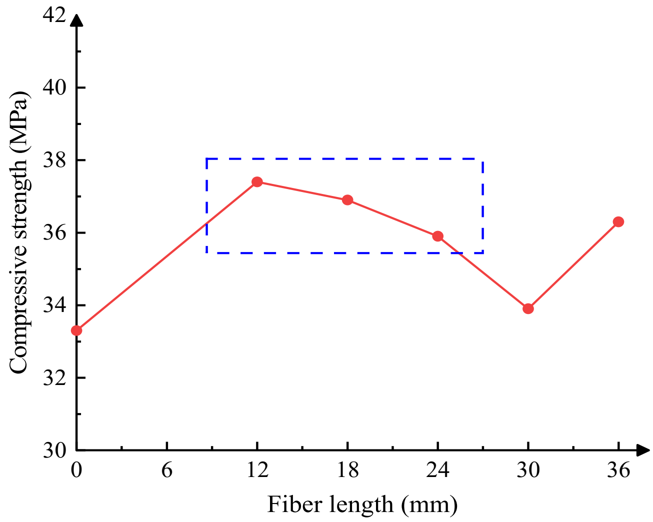

Figure 2. The 28 d compressive strength of the BRFC with different fiber lengths.

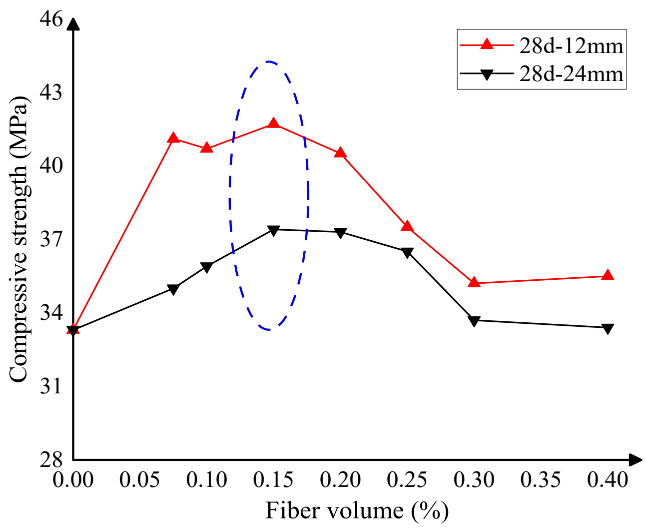

Figure 3. The compressive strength of the BRFC with different fiber volume contents.

4. Axial Compression Test of the BRFC Short Columns

4.1. Specimen Design

The analysis results of optimal design parameters in the previous section show that the optimal fiber length is 12–24 mm and the fiber volume content is 0.15%. As a result, in the subsequent experiments, only two fiber lengths of 12 mm and 18 mm, as well as fiber volume of 0.15%, are selected for the short column design. Here, a total of nine reinforced concrete short columns numbered S1–S9 are designed. Among them, the samples numbered S1–S3 are ordinary reinforced concrete short columns, and the samples numbered S4–S6 and S7–S9 are the BRFC short columns with fiber length of 12 mm and 18 mm, respectively. For all the BRFC short columns, the fiber volume content is selected as 0.15%, as previously described. The short column is featured with a cross-section size of width × height = 150 mm × 150 mm, and a slenderness ratio of 3.67 (length/width = 550/150 = 3.67), which is less than 8. The concrete cover is 10 mm. All short columns are arranged with four HRB400 threaded bars with a diameter of 12 mm as longitudinal reinforcement, and the stirrups are made of HRB335 plain round bars with a diameter of 6 mm and a spacing of 110 mm. The reinforcement configuration is provided in Figures 4 and 5. As required by GT/B 288.1-2010 [25], the yield and tensile strength of the two kinds of reinforcement are 486 MPa versus 360.1 MPa, and 590 MPa versus 570.4 MPa, respectively. Preloading is required before formal loading. Each short column is preloaded with 100 kN for 5 min to observe the reliability of the loading system and each measuring point. The formal loading is performed by the grading loading system. The loading of each stage is 50 kN, which is maintained for 2 min. When cracks or bulges appear, the loading is increased to 10 kN until the short column is damaged.

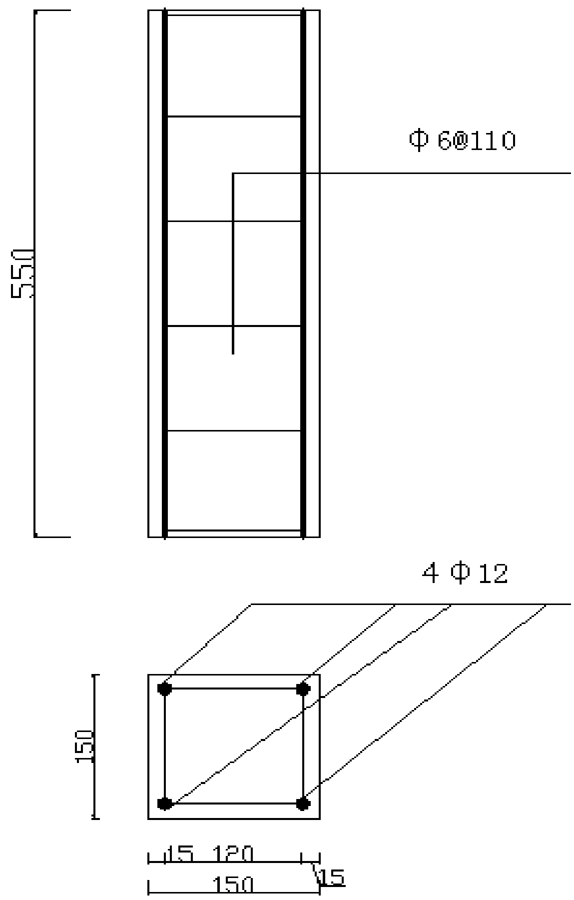

Figure 4. The structural dimension of the short column.

4.2. Experimental Phenomenon

During the loading process of all test short columns, no transverse cracks are found, while vertical cracks occur before failure. With the increase of load, the cracks develop gradually, the steel bars yield gradually, and the concrete is crushed and damaged. However, the stirrups remain intact when the short columns are damaged. The results reveal that the cracking of the BRFC short columns is significantly later than the ordinary RC short columns, which is also true for the failure load. The failure modes of the test specimens are shown in Figure 6.

Figure 5. The reinforcement of the short column.

(**a**)

(**b**)

(**c**)

(**d**)

(**e**)

(**f**)

Figure 6. *Cont*.

Figure 6. The failure mode of the short columns: (**a**) S1; (**b**) S2; (**c**) S3; (**d**) S4; (**e**) S5; (**f**) S6; (**g**) S7; (**h**) S8; and (**i**) S9.

4.3. Results and Discussion

4.3.1. Ultimate Bearing Capacity

It can be seen in Table 5 that the ultimate bearing capacity (N_u) of the BRFCthe BRFC short columns is significantly higher than ordinary RC short columns. In particular, the maximum increase rate of axial compression ultimate bearing capacity is 28% for the BRFC short columns with fiber length of 12 mm and is 20% for the BRFC short columns with a fiber length of 18 mm. The average increase is 24%. The results highlight that basalt fiber is beneficial to the ultimate bearing capacity of reinforced concrete short columns. In addition, the average value of the ultimate bearing capacity of the BRFC short columns with a fiber length of 12 mm is 636.7 kN, which is 6.7% higher than the corresponding value (596.7 kN) with a fiber length of 18 mm. This conclusion matches the conclusion in Section 3.2 and other types of fibers reported in [26,27]. That is, when the fiber length exceeds a certain value, the reinforcement effect of the fibers will weaken.

Table 5. The axial compression test results of the BRFC short columns.

Specimen Number	Fiber Volume Content (%)	Fiber Length (mm)	N_u (kN)
S1	0	/	500
S2	0	/	500
S3	0	/	490
S4	0.15	12	640
S5	0.15	12	640
S6	0.15	12	630
S7	0.15	18	600
S8	0.15	18	590
S9	0.15	18	600

4.3.2. Load Strain Curve

The average value of the measured strain of the concrete and steel bar at the midpoint of each column is plotted in Figures 7 and 8. As indicated, the short columns are basically in the elastic stage at the beginning of loading and then enter the elastic–plastic stage with the increase of load. The concrete strain of the S1–S3 short columns reaches its peak around 0.0019, compared to a peak of around 0.0021 for the S4–S6 short columns. For the S7–S9 short columns, the peak value is about 0.0023. In addition to a slightly larger steel strain at peak value, the slope of the N-ε curve of the BRFC short columns in the elastic stage is also greater than that of the reinforced concrete short column.

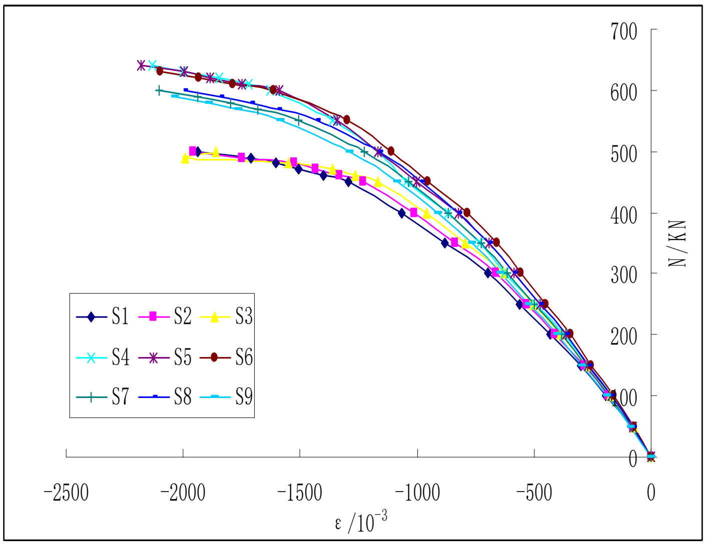

Figure 7. The average strain curve of the steel bars.

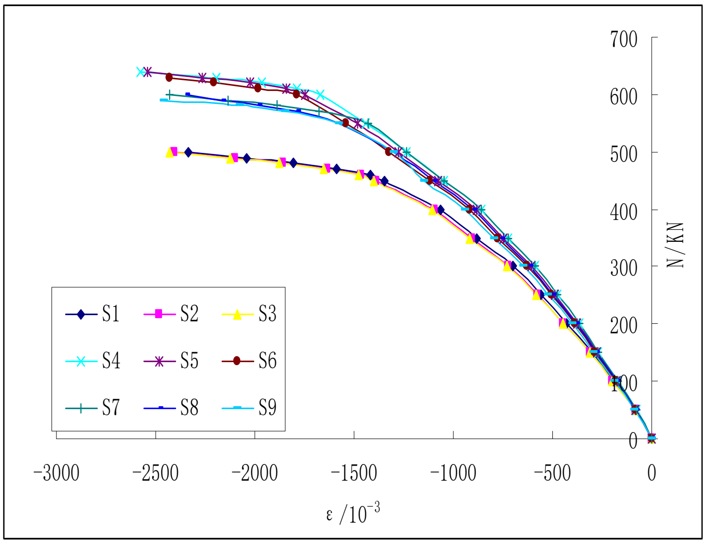

Figure 8. The average strain curve of the concrete.

Figure 9 shows the variation law of the vertical displacement at the top of each test short column. As indicated, the vertical displacement of the short column exhibits an obvious plastic stage with the increase of the load. The vertical displacement of the BRFC short columns is significantly greater than that of the ordinary RC short columns. More specifically, the vertical displacement of S4–S6 is the largest, followed by S7–S9, and is the smallest in S1–S3. Due to the restraint of fiber, the BFRC short column has greater displacement when the load reaches the peak value. From the elastic stage to elastic–plastic stage, the load displacement curve of the BRFC short columns is smoother and the plastic characteristics are obvious.

4.3.3. Influence Mechanism of Basalt Fiber

The chopped continuous basalt fiber is a hydrophilic material, which can be well combined with the cement-based material and form a spatial network structure between the concrete coarse aggregates. The structure encases the coarse aggregate and acts as a hindrance to aggregate movement during compression. Due to its high tensile strength, basalt fiber can provide circumferential restraint to resist transverse expansion when the specimen is compressed. As a result, its existence hinders the generation of a large number of microcracks or crosses countless microcracks. This makes the generation and development of cracks in the compression process require more energy. Thus, compared with the RC short columns, the ultimate bearing capacity of the BRFC short columns is significantly improved, and the initial crack time is also delayed. At the same time, when the basalt fiber concrete is equipped with an appropriate amount of stirrup and protective layer thickness, the anchorage ductility of the BRFC can be significantly increased. For the above reasons, the BFRC short column has higher ultimate bearing capacity and stronger deformation capacity.

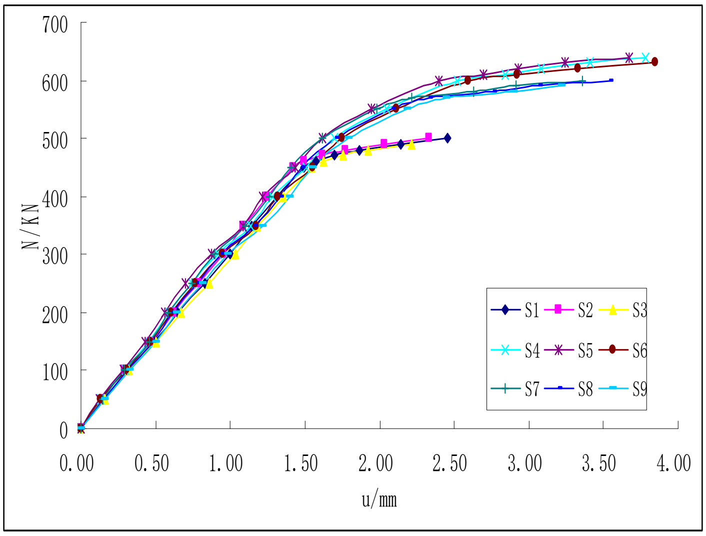

Figure 9. The load and the vertical displacement.

5. Calculation Method of Ultimate Bearing Capacity of BRFC Short Column

(1) Calculation method based on Standard approximate formula

In the specifications for the design of highway reinforced concrete and prestressed concrete bridges and culverts [28], the effect of the slenderness ratio is considered by solving the given calculation formula based on the sum of the maximum bearing capacity of concrete and steel bar. For the short columns with a rectangular cross-section, the calculation formula is as follows [28]:

$$N_u = 0.9\varphi(f_{cd}A + f'_{sd}A'_s) \quad (1)$$

where f_{cd} is the design value of the compressive strength of concrete, f'_{sd} is the design value of the yield strength of longitudinal reinforcement, A is the gross area of the cross section of a column, and A'_s is the area of longitudinal reinforcement. φ is the stability coefficient. The values or calculation methods of previous variables can be found in [28].

For the calculation of ultimate bearing capacity of the BRFC short column, the design value of concrete axial compressive strength in Equation (1) is replaced by the measured value of the compressive strength of the BRFC, and the other parameters remain unchanged. The calculation results are listed in Table 6.

(2) Finite element analysis method

The concrete constitutive model provided in [29] is adopted to calculate the ultimate bearing capacity of the BRFC short column, in which the peak strain, rising, and falling curves are modified by the measured strength of the BRFC. Moreover, considering the structural damage under the concrete stress, the elastic stiffness matrix is reduced and the correlation hardening is introduced into the constitutive model for the damage model of the ABAQUS software (version: 6.14.2), so as to better simulate the elastic–plastic behavior of the concrete in the loading. The C3D8R solid element and the T3D2 truss element are used for model concrete and reinforcement, respectively. The reference points are connected with the upper and lower surfaces by coupling. One end reference point is utilized to apply loads (with only one translational degree of freedom in the longitudinal direction of the column reserved), and another end reference point is used for boundary conditions (rigid junction). The reinforced concrete is connected by an embedded region and subject to load by a reference point according to the displacement. The point set is arranged at the loading point to facilitate reading the load in post-processing. A set of points is arranged at the core concrete to observe the relationship between the stress, the strain, and the load of the core concrete. The finite element model of the short column is illustrated in Figure 10, and the calculation results based on the finite element method are also shown in Table 6.

Table 6. The calculation value of the ultimate bearing capacity of the BRFC short column.

Specimen Number	Test Value (kN)	Calculation Value Based on Equation (1) (kN)	Calculation Value Based on Finite Element Analysis Method (kN)	η_1	η_2
S1	500	502	497	1.00	1.01
S2	500	502	497	1.00	1.01
S3	490	502	497	0.98	0.99
S4	640	630	637	1.02	1.00
S5	640	630	637	1.02	1.00
S6	630	630	637	1.00	0.99
S7	600	598	597	1.00	1.01
S8	590	598	597	0.99	0.99
S9	600	598	597	1.00	1.01

Note: η_1 = the ratio of the test value to the calculation value based on Equation (1); η_2 = the ratio of the test value to calculation value by the finite element analysis method.

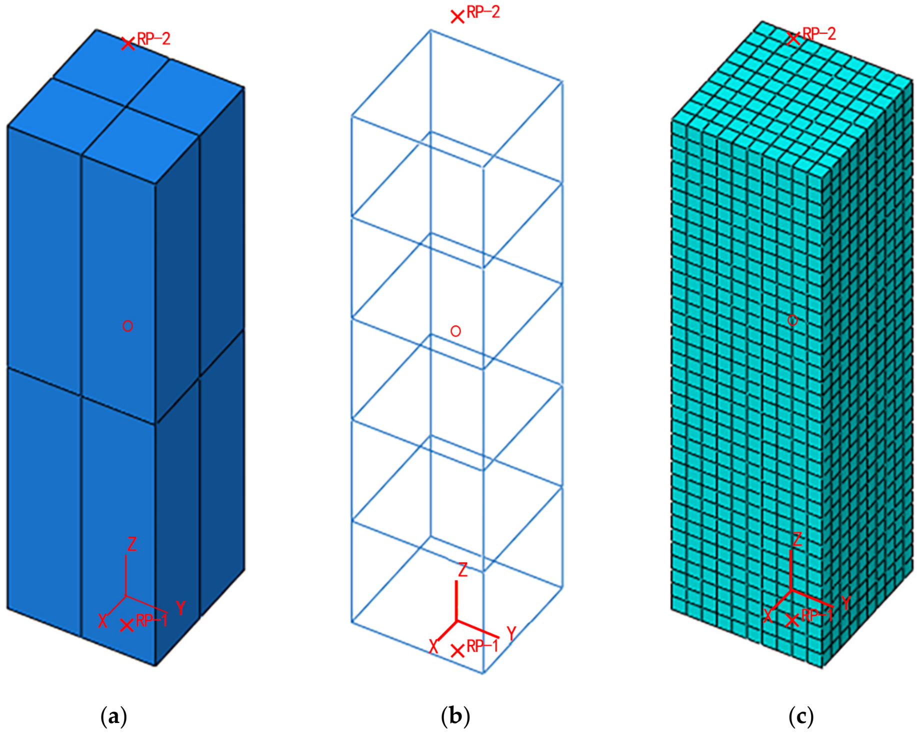

Figure 10. The finite element model of the short column: (**a**) the entity model; (**b**) the reinforcing element; and (**c**) the concrete unit.

As shown in Table 6, no matter which of the theoretical calculation methods based on the specification (i.e., Equation (1)) and the finite element simulation method is adopted, its calculation results are very consistent with the test results. More specifically, for the theoretical calculation method based on the specification, the calculated results of bearing capacity of the BRFC short columns are slightly lower than the measured values, while the corresponding results of the ordinary concrete short columns are slightly higher than the measured values. For the finite element simulation method, the calculation results of the BRFC and ordinary concrete short columns are mostly lower than the measured values. Although there is a certain deviation between the calculated results and the measured values, the maximum deviation is no more than 5%. This also verifies the feasibility of the bearing capacity prediction method of the BRFC short columns obtained by bringing the stress–strain relationship obtained from the test into the specification formula and the proposed finite element method. It is worth noting that due to the loading method of increasing 10 kN each time during the bearing capacity test of the concrete short columns (as described in Section 4.1), there is a certain deviation between the measured bearing capacity from the test and the actual bearing capacity of the concrete short columns. However, the deviation caused by this loading method is estimated to be between 1.5% and 2%. Therefore, it will not have a substantial impact on the effectiveness of the previous prediction methods.

6. Conclusions

In this paper, we obtained the optimum fiber length and fiber volume content based on the construction performance and the concrete compressive strength. The experimental phenomenon, the ultimate bearing capacity, the load strain curve, and the influence mechanism of basalt fiber are analyzed based on the results of the axial compression test of the BRFC short columns. In addition, the theoretical and finite element calculation method of the ultimate bearing capacity of the BRFC short column is proposed. The conclusions are summarized as follows:

(1) The optimum fiber length is about 12–24 mm, and the fiber volume content is 0.15%. In this case, the concrete has better slump and expansion properties and higher compressive strength.
(2) Adding appropriate basalt fiber can effectively improve the ultimate bearing capacity of the concrete short columns, and the maximum and average increases are 28% and 24%, respectively.
(3) No matter which of the theoretical calculation methods and the finite element simulation methods is adopted, its calculation results are very consistent with the test results. Even considering the deviation caused by the loading mode, the maximum deviation between the calculated results and the measured values is no more than 5%.

The limitation of this study is that only one diameter of basalt fiber is considered. In future research, the effect of the fiber diameter on the construction and mechanical properties of concrete needs to be further studied. Moreover, obtaining more measured data on the ultimate bearing capacity of the BRFC short columns to verify the effectiveness of the prediction method is also the focus of future research.

Author Contributions: Conceptualization, X.W.; methodology, X.W., R.Y. and P.L.; software, X.W.; validation, X.W. and Y.Y.; writing—original draft preparation, X.W. and Y.Y.; writing—review and editing, X.W., Y.Y., R.Y. and P.L.; supervision, R.Y. and P.L.; and funding acquisition, X.W., Y.Y. and R.Y. All authors have read and agreed to the published version of the manuscript.

Funding: This research was funded by the Hunan Provincial Natural Science Foundation of China (Grant Nos. 2021JJ50153, 2022JJ40024, and 2021JJ50156) and the Research Foundation of Education Bureau of Hunan Province (Grant Nos. 18A401, 21B0723, and 19C0343).

Institutional Review Board Statement: Not applicable.

Informed Consent Statement: Not applicable.

Data Availability Statement: Not applicable.

Acknowledgments: We would like to thank the anonymous reviewers and the editor for their valuable comments and remarks, which helped us to improve the original manuscript.

Conflicts of Interest: The authors declare that they have no known competing financial interests or personal relationships that could have influenced the work reported in this paper.

References

1. Iqbal, S.; Ali, A.; Holschemacher, K.; Bier, T.A. Mechanical properties of steel fiber reinforced high strength lightweight self-compacting concrete (SHLSCC). *Constr. Build. Mater.* **2015**, *98*, 325–333. [CrossRef]
2. Xin, H.; Liu, Y.; Mosallam, A.S.; He, J.; Du, A. Evaluation on material behaviors of pultruded glass fiber reinforced polymer (GFRP) laminates. *Compos. Struct.* **2017**, *182*, 283–300. [CrossRef]
3. Shaikh, F.U.A. Review of mechanical properties of short fibre reinforced geopolymer composites. *Constr. Build. Mater.* **2013**, *43*, 37–49. [CrossRef]
4. Hannawi, K.; Bian, H.; Prince-Agbodjan, W.; Raghavan, B. Effect of different types of fibers on the microstructure and the mechanical behavior of ultra-high performance fiber reinforced concretes. *Compos. Part B Eng.* **2016**, *86*, 214–220. [CrossRef]
5. Santarelli, M.L.; Sbardella, F.; Zuena, M.; Tirillo, J.; Sarasini, F. Basalt fiber reinforced natural hydraulic lime mortars: A potential bio-based material for restoration. *Mater. Des.* **2014**, *63*, 398–406. [CrossRef]
6. Bai, Y.; Nguyen, T.C.; Zhao, X.L.; Al-Mahaidi, R. Environment-assisted degradation of the bond between steel and carbon-fiber-reinforced polymer. *J. Mater. Civ. Eng.* **2014**, *26*, 04014054. [CrossRef]
7. Alabduljabbar, H.; Alyousef, R.; Mohammadhosseini, H.; Topper, T. Bond behavior of cleaned corroded lap spliced beams repaired with carbon fiber reinforced polymer sheets and partial depth repairs. *Crystals* **2020**, *10*, 1014. [CrossRef]
8. Meyyappan, P.L.; Carmichael, M.J. Studies on strength properties of basalt fiber reinforced concrete. *Mater. Today Proc.* **2021**, *43*, 2105–2108. [CrossRef]
9. Ramesh, B.; Eswari, S. Mechanical behaviour of basalt fibre reinforced concrete: An experimental study. *Mater. Today Proc.* **2021**, *43*, 2317–2322. [CrossRef]
10. Alaskar, A.; Albidah, A.; Alqarni, A.S.; Alyousef, R.; Mohammadhosseini, H. Performance evaluation of high-strength concrete reinforced with basalt fibers exposed to elevated temperatures. *J. Build. Eng.* **2021**, *35*, 102108. [CrossRef]
11. Branston, J.; Das, S.; Kenno, S.Y.; Taylor, C. Mechanical behaviour of basalt fibre reinforced concrete. *Constr. Build. Mater.* **2016**, *124*, 878–886. [CrossRef]
12. Wang, X.Z.; He, J.; Mosallam, A.S.; Li, C.; Xin, H. Effects of fiber length and volume on material properties and crack resistance of basalt fiber reinforced concrete (BFRC). *Adv. Mater. Sci. Eng.* **2019**, *4*, 7520549. [CrossRef]
13. Li, J.J.; Niu, J.G.; Wan, C.J.; Ling, X.Q.; Jin, Z.Y. Comparison of flexural property between high performance polypropylene fiber reinforced lightweight aggregate concrete and steel fiber reinforced lightweight aggregate concrete. *Constr. Build. Mater.* **2017**, *157*, 729–736. [CrossRef]
14. Ayub, T.; Shafifiq, N.; Khan, S.U. Compressive stress-strain behavior of HSFRC reinforced with basalt fibers. *J. Mater. Civ. Eng.* **2015**, *28*, 06015014. [CrossRef]
15. Wang, H.L.; Yuan, L.; Song, H. Experimental study on mechanical property of chopped basalt fiber reinforced concrete. *Build. Struct.* **2013**, *43*, 562–564.
16. Monaldo, E.; Nerilli, F.; Vairo, G. Basalt-based fiber-reinforced materials and structural applications in civil engineering. *Compos. Struct.* **2019**, *214*, 246–263. [CrossRef]
17. Sun, X.J.; Gao, Z.; Cao, P.; Zhou, C.J. Mechanical properties tests and multiscale numerical simulations for basalt fiber reinforced concrete. *Constr. Build. Mater.* **2019**, *202*, 58–72. [CrossRef]
18. Tumadhir, M. Thermal and mechanical properties of basalt fibre reinforced concrete. *Int. J. Civ. Environ. Eng.* **2013**, *7*, 334–337.
19. Zhang, Y. *Research on Basic Mechanical Properties of Chopped Basalt Fiber Reinforced Concrete*; Northeast Forestry University: Harbin, China, 2011.
20. Wang, J.; Luan, Y.; Ye, H.J. Experimental research on crack and deformation of basalt fiber reinforced concrete beams. *J. Archit. Civ. Eng.* **2016**, *33*, 76–81.
21. Alnahhal, W.; Aljidda, O. Flexural behavior of basalt fiber reinforced concrete beams with recycled concrete coarse aggregates. *Constr. Build. Mater.* **2018**, *169*, 165–178. [CrossRef]
22. Zhu, C.R. *Experimental Study on Fatigue of Basalt Fiber Reinforced Concrete Beams*; Inner Mongolia University of Technology: Hohhot, China, 2013.
23. *GB/T 50080-2016*; Standard for Test Method of Performance on Ordinary Fresh Concrete. MOHURD: Beijing, China, 2016.
24. *GB/T 50081-2002*; Standard for Test Method of Mechanical Properties on Ordinary Concrete. MOHURD: Beijing, China, 2002.
25. *GT/B288.1-2010*; Metallic Materials-Tensile Testing—Part 1, Method of Test at Room Temperature. National Technical Committee for Steel Standardization: Beijing, China, 2010.
26. Abirami, R.; Sangeetha, S.P. Study on fiber reinforced concrete beam-column connection—A review. *Mater. Today Proc.* **2020**, *33*, 415–419. [CrossRef]
27. Yoo, D.Y.; Banthia, N. Mechanical properties of ultra-high-performance fiber-reinforced concrete: A review. *Cem. Concr. Comp.* **2016**, *73*, 267–280. [CrossRef]
28. *JTG 3362-2018*; Specifications for Design of Highway Reinforced Concrete and Prestressed Concrete Bridges and Culverts. MOT: Beijing, China, 2018.
29. Shao, X.D.; Fan, W.; Huang, Z.Y. Application of ultra-high-performance concrete in engineering structures. *China Civ. Eng, J.* **2021**, *54*, 1–13.